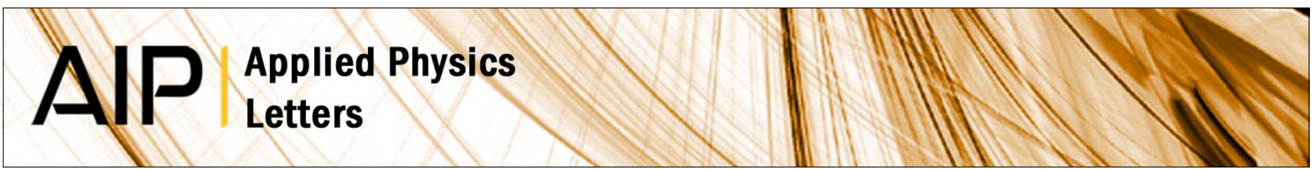

Phase and thickness dependent modulus of Ge2Sb2Te5 films down to 25 nm thickness

Yoonjin Won, Jaeho Lee, Mehdi Asheghi, Thomas W. Kenny, and Kenneth E. Goodson

Citation: Appl. Phys. Lett. **100**, 161905 (2012); doi: 10.1063/1.3699227
View online: http://dx.doi.org/10.1063/1.3699227
View Table of Contents: http://apl.aip.org/resource/1/APPLAB/v100/i16
Published by the American Institute of Physics.

Related Articles

Dynamic nanomechanics of zinc oxide nanowires
Appl. Phys. Lett. 100, 163110 (2012)

Surface elasticity effect on the size-dependent elastic property of nanowires
J. Appl. Phys. 111, 083506 (2012)

Nonlinear viscoelasticity of freestanding and polymer-anchored vertically aligned carbon nanotube foams
J. Appl. Phys. 111, 074314 (2012)

Surface polar states and pyroelectricity in ferroelastics induced by flexo-roto field
Appl. Phys. Lett. 100, 142902 (2012)

Strain relaxation in single crystal SrTiO3 grown on Si (001) by molecular beam epitaxy
J. Appl. Phys. 111, 064112 (2012)

Additional information on Appl. Phys. Lett.

Journal Homepage: http://apl.aip.org/
Journal Information: http://apl.aip.org/about/about_the_journal
Top downloads: http://apl.aip.org/features/most_downloaded
Information for Authors: http://apl.aip.org/authors

ADVERTISEMENT

Downloaded 18 Apr 2012 to 171.67.216.23. Redistribution subject to AIP license or copyright; see http://apl.aip.org/about/rights_and_permissions

Phase and thickness dependent modulus of $Ge_2Sb_2Te_5$ films down to 25 nm thickness

Yoonjin Won, Jaeho Lee, Mehdi Asheghi, Thomas W. Kenny, and Kenneth E. Goodson
Department of Mechanical Engineering, Stanford University, Stanford, California 94305, USA

(Received 1 February 2012; accepted 24 February 2012; published online 18 April 2012)

The mechanical properties of phase-change materials including $Ge_2Sb_2Te_5$ (GST) are strongly influenced by the complex interaction of phase and imperfection distributions, especially at film thicknesses relevant for phase-change memory devices. This work uses a micromechanical resonator as a substrate to study the phase dependent modulus of GST films with thicknesses from 25 nm to 350 nm. The moduli of amorphous GST and crystalline GST films increase with decreasing thickness to 10 GPa and up to 60 GPa, respectively. The phase purity is studied using X-ray diffraction and energy dissipation data, which provide qualitative information about inelastic absorption. © *2012 American Institute of Physics*. [http://dx.doi.org/10.1063/1.3699227]

Phase-change memory (PCM) is a promising data storage technology[1,2] with performance metrics governed by complex thermal, electrical, and mechanical phenomena. A phase change material, such as $Ge_2Sb_2Te_5$ (GST), switches between amorphous and crystalline phases and experiences temperature excursions exceeding 600 °C. The thermal expansion mismatch between the GST and the surrounding materials causes severe mechanical stresses, which can lead to delamination failure.[3] The phase dependent mechanical modulus of GST influences interfacial stresses and failure onset.[4] Many of the previous measurements of the GST modulus used nanoindentation to compress the film in the out-of-plane direction or a wafer curvature technique. As the dimensions of phase change memory devices are reduced, the impact of interfaces or grain sizes on the properties is expected to increase. This has motivated research on GST films as thin as 60 nm.[5] There is a need for data on thinner films both to reflect the very small device geometries and to support a deeper understanding of the physics governing the thickness dependent mechanical properties.

In this letter, we report measurements of the elastic modulus of GST films down to 25 nm using a micromechanical resonating beam as a sensor of the properties of films deposited on the beam. A laser Doppler vibrometer (LDV) captures the resonant frequency shift induced by deposition of a thin film.[6] The resonant frequency shift is used to calculate the elastic modulus of GST films of varying film thickness. In addition, we monitor the exponential decay in the amplitude of the vibration after removal of the stimulus to calculate the energy storage factor of these Si-GST composite cantilevers.[7] The energy storage factor of GST films is separated from that of the composite cantilever and is used along with X-ray diffraction (XRD) data to understand the role of grain size and phase purity.

The fabrication process of these microcantilevers uses SOI wafers and standard etching procedures, and they are detailed elsewhere.[6] The ratios of cantilever length (600–1000 μm) to thickness (6 μm) are varied to achieve a range of resonant frequencies. The amorphous-GST films, in the range of 25–350 nm, are sputter-deposited on these microfabricated cantilevers at room temperature. Annealing of the films after deposition to temperatures of 150, 300, and 400 °C leads to different levels of crystallization, and detectable changes in the resonant frequency and energy loss in these cantilevers.

The LDV measurement extracts the mechanical properties of GST film by measuring the resonant frequency change before and after the film deposition, as illustrated in the inset of Fig. 1. The ratio of the resonant frequency shift after the film deposition to the original resonant frequency of a silicon-only cantilever, Δ, enables us to extract the elastic modulus of the GST film using Eq. (1),

$$E_{GST} = \frac{E_{Si}}{I_{GST}}\left(\left(1+\frac{(\rho A)_{GST}}{(\rho A)_{Si}}\right)(1+\Delta)^2 I_{Si,0} - I_{Si}\right), \quad (1)$$

where E, I, ρ, and A, are, respectively, the modulus, the second moment of area, density, and cross-sectional area.[8,9] The subscripts, $Si,0$, Si, and GST denote the silicon layer of a silicon-only cantilever, the silicon, and GST layer of a

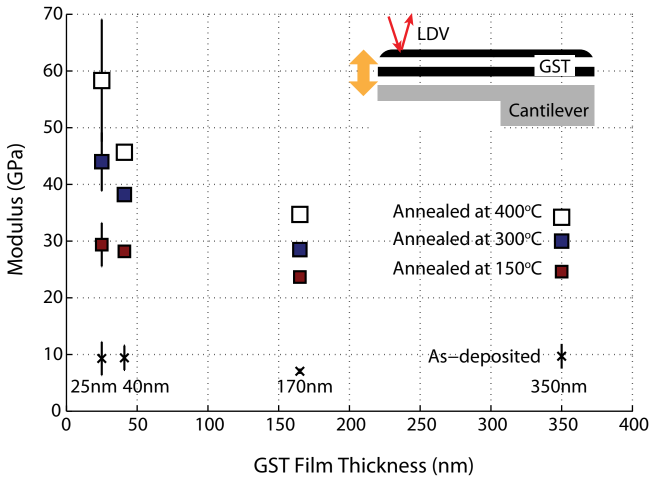

FIG. 1. Elastic modulus of as-deposited and annealed GST films. Samples include film thicknesses of 25, 40, 170, and 350 nm from four separate depositions. Squares and error bars are representing the averages and standard deviations of modulus values, respectively. (Inset) Schematic of a Si-GST composite cantilever and the LDV instrument used for measurement of cantilever vibration.

 © 2012 American Institute of Physics

Downloaded 18 Apr 2012 to 171.67.216.23. Redistribution subject to AIP license or copyright; see http://apl.aip.org/about/rights_and_permissions

Si-GST composite cantilever, respectively. The frequency shift ratios of 0.3%–0.5% are captured for the 25 nm-thick GST films. The higher frequency shift ratios of 4%–6% are obtained for the 350 nm-thick GST films. The resulting resonant frequency shifts range from 50 to 100 Hz up to 6 kHz, where the measurement resolution of 1.25 Hz is small enough to detect the minimum resonant frequency shift.

The different phases of the GST films exhibit different rates of energy dissipation. To extract the quality factor of a cantilever, we abruptly stop the driving signal at the steady state and record the resulting decay of the vibrational amplitude, which gives us the quality factor ($Q = \pi\tau_0 f_{res}$) of the structure, where f_{res} is the resonant frequency, and τ_0 is the time constant for decay of an oscillation. An example of ring-down measurement signal is shown in the inset of Fig. 5. The ring-down measurement before and after deposition of the GST film enables us to quantify the contribution of GST films to the energy storage factor of Si-GST films using

$$Q_{GST} = \left(\frac{1+\beta}{Q_{Si-GST}} - \frac{\beta}{Q_{Si}} \right)^{-1}, \tag{2}$$

where $\beta = (EI)_{Si}(EI)_{GST}^{-1}$. Many individual mechanisms may contribute to determine the energy storage factor of GST films, $Q_{\rm GST}$, according to[7]

$$\frac{1}{Q_{GST}} = \frac{1}{Q_{air}} + \frac{1}{Q_{TED}} + \frac{1}{Q_{viscoelastic}} + \frac{1}{Q_{anchor}} + \frac{1}{Q_{surface}} + \frac{1}{Q_{others}}. \tag{3}$$

In this equation, the dominant energy loss mechanism is often the energy loss due to collisions with the surrounding gas. When the experiments are executed in vacuum, air damping can be neglected. Another known loss mechanism in micromechanical resonators is thermoelastic dissipation (TED). In these experiments, we neglect TED in the GST films because TED depends on weak coupling between thermal and mechanical phenomena in solid films and is probably not a significant source of energy loss in these disordered GST films. Instead, we assume that the viscoelastic-limited factor, $Q_{\rm viscoelastic}$, dominates the total energy storage factor of the film and is strongly dependent on the structure of the GST film. Therefore, the total energy storage factor gives a means of characterizing the crystal structures of the GST films.

Mechanical property differences in thin films can result from their microstructures and crystallization details. In our experiments, annealing is carried out at 150, 300, and 400 °C for 10 min to produce different crystalline states, such as face centered cubic (*fcc*) and/or hexagonal close packed (*hcp*) phases. The crystallization of GST films, a type of nucleation dominated-growth, increases the grain sizes and rearranges the atomic structures as well. Because of enlarged grain sizes, the grain boundaries occupy a smaller fraction of the total volume in films, which gives rise to a more dense film with a higher modulus. The crystallization process with higher annealing temperature increases nucleation growth rates as well as the grain sizes.[10] Therefore, crystallization caused by high annealing temperatures increases the modulus of crystalline GST film, as indicated in Fig. 1. This phase transformation is also accompanied by considerable reduction in film thicknesses due to the change in density. The thickness decrease of 5%–8% is observed for crystalline GST films by using a profilometer (Dektek). The film thicknesses and mass densities (5.0–6.2 g/cm^3) of GST films are reconfirmed using the X-ray reflectometry (XRR; PANalytical X'Pert PRO).

For data interpretation, the largest source of uncertainty comes from the thickness and density variations. We minimize this uncertainty by confirming the thickness and density using a profilometer and XRR. The thickness measurement is accurate to 1%–2%, and the density measurement is accurate to 2%. For the thinnest films, the thickness nonuniformity along the cantilever has a stronger impact on the uncertainty of modulus calculation. Thus, the combined uncertainty in the determination of the modulus of thin films is up to 30%, whereas the thick films have an uncertainty of only 1%–2%.

Another difference between nominally identical as-deposited GST films can come from variations in deposition conditions. This work varies GST film thickness where ideally only the growth time varies between runs. However, it is difficult to maintain the identical temperature and pressure in each run, resulting in variations between our own samples. With respect to the uncertainty ranges of the measurement, the measured moduli of as-deposited GST films exhibit weak thickness dependence, whereas the moduli of crystalline GST films increase with decreasing film thickness. The increase in modulus of crystalline GST films may be explained with the (1) stiffening effect, (2) crystallization temperature, and (3) anisotropy of the columnar grain structures and phase impurities.

For the thinnest nanostructured films, a significant variation of mechanical properties can be observed due to the high surface-to-volume ratio. Cao *et al.*[11] adopted a molecular mechanics method to simulate atomic interactions within ZnO nanofilms, and their results imply that the modulus increases with the reduction of nanofilm thickness. In his paper, the variations in bond structures were observed leading to residual tension in interior films. The increased residual tension stiffens the film, resulting in a high modulus, which is known as the stiffening effect.

A number of studies indicate that the crystallization temperature and the impact of annealing time are different for films below 50 nm in thickness.[12–15] Depending on the interface energy difference between the GST film and the surrounding materials, the crystallization temperature can increase or decrease with decreasing film thickness. Because of the similarity of substrates in Peng *et al.*[13] and our films, the crystalline quality of the 25-nm-thick GST film should be better than that of thicker films. This argument is supported by our past measurements of the *Seebeck* coefficient and the electrical resistivity, where weaker electron scattering in the 25-nm-thick GST film was observed.[12]

The grain structures and phase impurities, revealed by transmission electron microscopy (TEM) images,[16] are also responsible for the observed variations in mechanical properties with thickness. The crystallization of GST films is triggered by nucleation at the interfaces and further elongates

Downloaded 18 Apr 2012 to 171.67.216.23. Redistribution subject to AIP license or copyright; see http://apl.aip.org/about/rights_and_permissions

grains in their thickness direction, leading to columnar grains.[16,17] Since the heights of the columnar grains are comparable to the thickness of thin GST films, the effects of the columnar grains on the modulus should be stronger for thin films. Several papers also reported that the properties correlate with the varying fraction of phase impurities,[18] where phase impurities decay exponentially with crystallization time following the Johnson-Mehl-Avrami-Kolmogrov model.[19] Our past work has consistently shown that the measurement results plateau as GST films are fully crystallized after a long annealing time, such as 30–60 min.[18] This means that an annealing time of 10 min may be not enough to crystallize the entire films, leading to phase impurities within thick GST films. Therefore, the variations in stiffening effects, crystallization temperatures, grain structures, and phase impurities may induce the higher modulus of 25 nm GST film than thick films.

Figure 2 shows the literature values of measured modulus for various film thicknesses. Numerous studies have measured the modulus of GST films using nanoindentation techniques.[20,21] However, nanoindentation measurements are not well-suited for thin films due to the strong influence of the substrate on the data. Nanoindentation measurements also require an assumed value for Poisson's ratio to calculate the elastic modulus of films. As a result, measured moduli using nanoindentation techniques are often higher than those using other techniques. Other studies have employed wafer curvature measurements interpreted using the Stoney equation.[5,20,22,23] The slopes of the stress and temperature curves give the mean of the average modulus by assuming the modulus would be temperature independent over the given temperature range. However, since as-deposited GST films are expected to change their mechanical modulus under heating, this approach overestimates the modulus. Therefore, the measured moduli using the wafer curvature technique are usually higher than those of the current work. Another uncertainty between the reported samples can come from various deposition conditions, which determine their grain structures as well as the mechanical properties. The density of our amorphous GST films, confirmed using XRR, ranges of 5.0–5.4 g/cm^3, which is less dense than the 5.8 g/cm^3 reported for other films.[20] Therefore, variations in the measurement techniques, deposition steps, film densities, and annealing process cause variability in the reported modulus of GST films. The modulus values of the current work are largely consistent with literature values. For most of our films, the elastic modulus of as-deposited GST films is much lower than that of bulk annealed crystalline GST films.

XRD measurements reveal the variation of the crystalline structures of GST films with annealing temperatures. A 125 nm-thick GST film, deposited using the sputtering technique, is annealed at 150, 300, and 400 °C. As depicted in Fig. 3, the as-deposited GST film is in the amorphous phase (grey line) showing no peaks in the XRD experiment. The film annealed at 150 °C for 10 min (navy line) exhibits a new peak, associated with appearance of the *fcc* phase. The film annealed at 300 °C for 10 min (orange line) exhibits both *fcc* and *hcp* phases. The film with additional annealing at 400 °C for 1 min (red line) shows a clear peak, indicating the hexagonal structures only (*hcp* phases).

These variations in crystalline structure can also be understood by studying the vibrational energy storage of the cantilevers carrying these GST films. The energy storage factors of silicon-only cantilevers (Q_{Si}) range from 20 000 to 40 000 with this variation arising because of variations in cantilever dimensions, as shown in Fig. 4. The deposition of the GST films at room temperature decreases the energy storage factors, to a range from 12 000 to 17 000. Initial annealing at 150 °C shows a small effect on the energy storage factor of Si-GST cantilevers. The second annealing at 300 °C increases the energy storage factor of Si-GST cantilevers by up to 20 000–30 000. This enhancement in energy storage factors indicates that the annealing at 300 °C lessens energy loss associated with grain boundaries and improves the film quality. The additional annealing at 400 °C shows relatively small increases in energy storage factors. The values of energy storage factors demonstrate that the energy dissipations are larger for amorphous GST films than other crystalline films and are consistent with our XRD result.

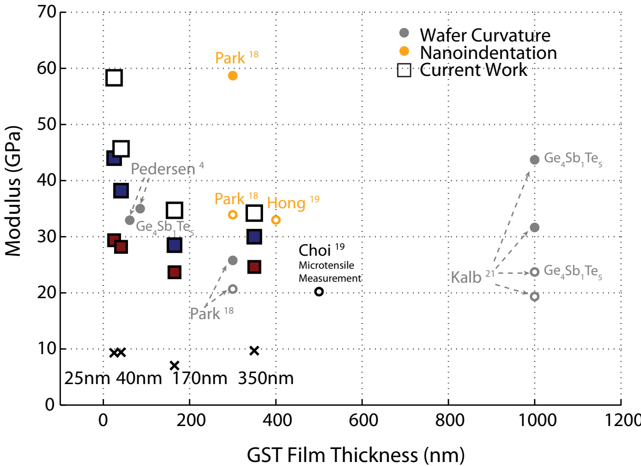

FIG. 2. Comparison of elastic moduli of amorphous and crystalline GST films as a function of the film thickness using literature values. The solid and empty circles illustrate crystalline and amorphous GST ($Ge_2Sb_2Te_5$ or $Ge_4Sb_1Te_5$ alloys), respectively.

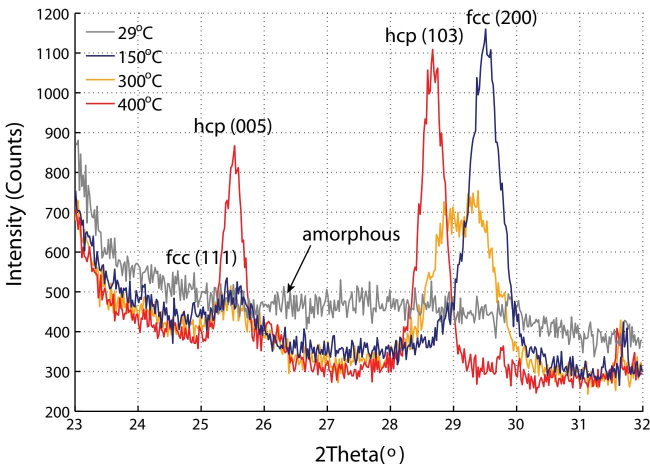

FIG. 3. X-ray diffraction scans of 125-nm-thick GST film on silicon substrates after different annealing procedures at 150, 300, and 400 °C using Cu Ka radiation.

Downloaded 18 Apr 2012 to 171.67.216.23. Redistribution subject to AIP license or copyright; see http://apl.aip.org/about/rights_and_permissions

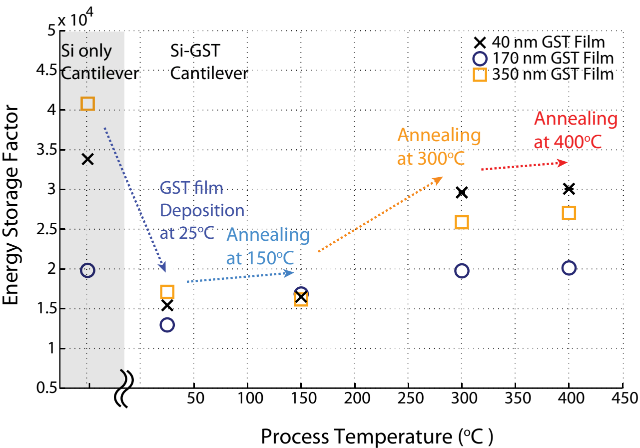

FIG. 4. Energy storage factors of silicon-only cantilevers and Si-GST cantilevers with 40, 170, and 350 nm-thick GST films are plotted. The energy storage factors in this paper are averages of multiple ring-down measurements for each cantilever.

We separate the energy storage factor of the GST films following Eq. (2), and the energy storage factor coefficient is defined as the contribution of the energy storage factor of a GST layer to that of the original silicon-only cantilever. The separated energy storage factors of as-deposited and crystalline GST films show reductions of 88%–99% relative to the energy storage factors of silicon-only cantilevers, as indicated in Fig. 5. The contribution of thin as-deposited GST films is smaller than the contribution of thick as-deposited GST films, leading to the smaller error bars in Fig. 5 for the thicker films. The initial annealing at 150 °C increases the energy storage factors of GST films by a factor of 1.5–7, and the additional annealing at 300 and 400 °C increases the energy storage factors by an additional factor of 6–17. Therefore, the crystallization process enhances the quality of all films, after which the energy storage factors of thin films are similar to those of thick films.

In this work, we characterize GST films with four different crystalline structures to investigate the phase and thickness dependent modulus of these films down to 25 nm. The elastic moduli of crystalline GST films are a factor of 3-4 higher than the corresponding amorphous values, and the energy storage factors are a factor of 2-3 higher than the corresponding amorphous values. The process of crystallization improves the film quality, as indicated by increases in the energy storage factors and increases in the mechanical modulus. The next goal of this study is to characterize the thermomechanical properties of GST films at high-temperatures up to 400 °C. Understanding of the impact of repetitive cycling on mechanical properties and mechanical failure would also enable improvement of the device performance and reliability, which are vital for application of PCM devices.

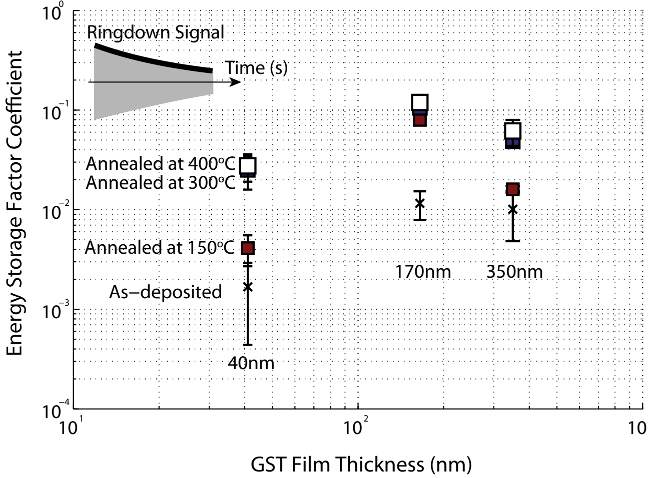

FIG. 5. Energy storage factor coefficients of GST films are plotted as a function of film thickness and annealing conditions. (Inset) Example of a ring-down measurement signal.

The authors would like to thank Dr. Kuo-Wei Chang for his helpful input. The authors appreciate the support from Intel Corporation, the Semiconductor Research Corporation through Contract No. 2009-VJ-1996, the National Science Foundation through Grant No. CBET-0853350, and the Office of Naval Research (ONR) Thermal Management Program through Contract No. N00014-09-1-0296-P00004. The authors also appreciate the support of the Stanford Nanofabrication Facility (SNF) and the Stanford Nanocharacterization Laboratory (SNL).

[1]H.-S. P. Wong, S. Raoux, S. Kim, J. Liang, J. P. Reifenberg, B. Rajendran, M. Asheghi, and K. E. Goodson, Proc. IEEE **98**, 2201 (2012).
[2]S. Raoux, Annu. Rev. Mater. Res. **39**, 25 (2009).
[3]J.-K. Ahn, K.-W. Park, N.-J. Seong, and S.-G. Yoon, J. Vac. Sci. Technol. B **27**, L54 (2009).
[4]Q. Guo, M. Li, Y. Li, L. Shi, T. C. Chong, J. A. Kalb, and C. V. Thompson, Appl. Phys. Lett. **93**, 221907 (2008).
[5]T. P. L. Pedersen, J. Kalb, W. K. Njoroge, D. Wamwangi, M. Wuttig, and F. Spaepen, Appl. Phys. Lett. **79**, 3597 (2001).
[6]Y. Won, Y. Gao, M. A. Panzer, S. Dogbe, L. Pan, T. W. Kenny, and K. E. Goodson, Carbon **50**, 347 (2012).
[7]R. N. Candler, A. Duwel, M. Varghese, S. A. Chandorkar, M. A. Hopcroft, W. T. Park, B. Kim, G. Yama, A. Partridge, and M. Lutz, J. Microelectromech. Syst. **15**, 927 (2006).
[8]I. Voiculescu, M. Zaghloul, and R. McGill, Proc. Inst. Mech. Eng. **220**, 1601 (2006).
[9]M. A. Hopcroft, W. D. Nix, and T. W. Kenny, J. Microelectromech. Syst. **19**, 229 (2010).
[10]S. Privitera, C. Bongiorno, E. Rimini, and R. Zonca, Appl. Phys. Lett. **84**, 4448 (2004).
[11]G. Cao and X. Chen, Int. J. Solids Struct. **45**, 1730 (2008).
[12]J. Lee, T. Kodama, Y. Won, M. Asheghi, and K. E. Goodson, Proceedings of the ASME 2012 3rd Micro/Nanoscale Heat & Mass Transfer International Conference, MNHMT, Atlanta, GA (2012).
[13]H. K. Peng, K. Cil, A. Gokirmak, G. Bakan, Y. Zhu, C. S. Lai, C. H. Lam, and H. Silva, Thin Solid Films **520**, 2976 (2012).
[14]S. Raoux, H.-Y. Cheng, J. L. Jordan-Sweet, B. Muñoz, and M. Hitzbleck, Appl. Phys. Lett. **94**, 183114 (2009).
[15]G. Bai, R. Li, H. N. Xu, Y. D. Xia, Z. G. Liu, H. M. Lu, and J. Yin, Physica B **406**, 4436 (2011).
[16]J. Lee, Z. Li, J. P. Reifenberg, S. Lee, R. Sinclair, M. Asheghi, and K. E. Goodson, J. Appl. Phys. **109**, 084902 (2011).
[17]S. W. Ryu, J. H. Oh, J. H. Lee, B. J. Choi, W. Kim, S. K. Hong, C. S. Hwang, and H. J. Kim, Appl. Phys. Lett. **92**, 142110 (2008).
[18]Z. Li, J. Lee, J. P. Reifenberg, M. Asheghi, R. G. D. Jeyasingh, H.-S. P. Wong, and K. E. Goodson, IEEE Electron Device Lett. **32**, 961 (2011).
[19]J. Farjas and P. Roura, Acta Mater. **54**, 5573 (2006).
[20]I. Park, J. Jung, S. Ryu, K. Choi, B. Yu, Y. Park, S. Han, and Y. Joo, Thin Solid Films **517**, 848 (2008).
[21]Y. Choi and Y.-K. Lee, Electron. Mater. Lett. **6**, 23 (2010).
[22]J.-H. Zhao, T. Ryan, P. S. Ho, A. J. McKerrow, and W.-Y. Shih, J. Appl. Phys. **88**, 3029 (2000).
[23]J. Kalb, F. Spaepen, T. Leervad Pedersen, and M. Wuttig, J. Appl. Phys. **94**, 4908 (2003).

Downloaded 18 Apr 2012 to 171.67.216.23. Redistribution subject to AIP license or copyright; see http://apl.aip.org/about/rights_and_permissions